Enhancing the Performance of HPAM Polymer Flooding Using Nano CuO/Nanoclay Blend

Authors:

Saket Kumar, Roshan Tiwari, Maen Husein, Nitesh Kumar, Upendra Yadav

Date Submitted: 2020-12-17

Keywords: rheology, CEOR, nanoclay, nanoparticle, nanohybrid, polymer flooding

Abstract:

A single polymer flooding is a widely employed enhanced oil recovery method, despite polymer vulnerability to shear and thermal degradation. Nanohybrids, on the other hand, resist degradation and maintain superior rheological properties at different shear rates. In this article, the effect of coupling CuO nanoparticles (NPs) and nanoclay with partially hydrolyzed polyacrylamide (HPAM) polymer solution on the rheological properties and the recovery factor of the nanohybrid fluid was assessed. The results confirmed that the NP agents preserved the polymer chains from degradation under mechanical, chemical (i.e., salinity), and thermal stresses and maintained good extent of entanglement among the polymer chains, leading to a strong viscoelastic attribute, in addition to the pseudoplastic behavior. The NP additives increased the viscosity of the HPAM polymer at shear rates varying from 10?100 s?1. The rheological properties of the nanohybrid systems varied with the NP additive content, which in turn provided a window for engineering a nanohybrid system with a proper mobility ratio and scaling coefficient, while avoiding injectivity issues. Sandpack flooding tests confirmed the superior performance of the optimized nanohybrid system and showed a 39% improvement in the recovery ratio relative to the HPAM polymer injection.

Record Type: Published Article

Submitted To: LAPSE (Living Archive for Process Systems Engineering)

Citation (overall record, always the latest version): LAPSE:2020.1188
Citation (this specific file, latest version): LAPSE:2020.1188-1
Citation (this specific file, this version): LAPSE:2020.1188-1v1

DOI of Published Version: https://doi.org/10.3390/pr8080907

processes

MDPI

Article

Enhancing the Performance of HPAM Polymer Flooding Using Nano CuO/Nanoclay Blend

Saket Kumar [1], Roshan Tiwari [2], Maen Husein [1,*], Nitesh Kumar [3] and Upendra Yadav [4]

1 Department of Chemical & Petroleum Engineering, University of Calgary, Calgary, AB T2N 1N4, Canada; saket.kumar1@ucalgary.ca
2 Department of Petroleum and Energy Studies, DIT University, Dehradun, Uttarakhand 248009, India; Roshan.dit16@gmail.com
3 MDNK Oil & Gas Consultants, Mumbai, Maharashtra 400001, India; nitesh5@hotmail.com
4 Department of Petroleum Engineering and Earth Sciences, University of Petroleum and Energy Studies, Dehradun, Uttarakhand 248001, India; yadavupend@gmail.com
* Correspondence: maen.husein@ucalgary.ca; Tel.: +(403)-220-6691; Fax: +(403)-282-3945

Received: 28 June 2020; Accepted: 22 July 2020; Published: 1 August 2020

Abstract: A single polymer flooding is a widely employed enhanced oil recovery method, despite polymer vulnerability to shear and thermal degradation. Nanohybrids, on the other hand, resist degradation and maintain superior rheological properties at different shear rates. In this article, the effect of coupling CuO nanoparticles (NPs) and nanoclay with partially hydrolyzed polyacrylamide (HPAM) polymer solution on the rheological properties and the recovery factor of the nanohybrid fluid was assessed. The results confirmed that the NP agents preserved the polymer chains from degradation under mechanical, chemical (i.e., salinity), and thermal stresses and maintained good extent of entanglement among the polymer chains, leading to a strong viscoelastic attribute, in addition to the pseudoplastic behavior. The NP additives increased the viscosity of the HPAM polymer at shear rates varying from 10–100 s^{-1}. The rheological properties of the nanohybrid systems varied with the NP additive content, which in turn provided a window for engineering a nanohybrid system with a proper mobility ratio and scaling coefficient, while avoiding injectivity issues. Sandpack flooding tests confirmed the superior performance of the optimized nanohybrid system and showed a 39% improvement in the recovery ratio relative to the HPAM polymer injection.

Keywords: polymer flooding; nanohybrid; nanoparticle; nanoclay; CEOR; rheology

1. Introduction

The demand on energy is growing with the increased population and improved lifestyle. In the meantime, the volume of oil produced under natural reservoir drives is declining [1]. Most oil reservoirs currently apply one or more improved oil recovery (IOR) mechanisms to boost their production [2]. IOR stimulates reservoir production by means of micro- and macroscopic sweep mechanisms [3]. Water/brine flooding is amongst the first alternatives to sustain reservoir production, owing to its relatively low cost [4]. Water flooding is generally used in light oil reservoirs owing to its high recovery factor, favorable mobility ratio, good sweep efficiency, suitability for long-term injection, and competitive cost [5]. Nevertheless, water flooding is ineffective for reservoirs of high oil viscosity [6]. The big disparity in the viscosities of the displacing phase (water) and the displaced phase (oil) induce viscous fingering, which leads to an unfavorable mobility ratio and early breakthrough of the displacing fluid [7]. Polymer flooding includes the addition of polymers to the brine as an attempt to bridge the disparity in viscosity between the injected and the reservoir fluids [4]. More favorable mobility ratios are therefore expected relative to brine injection [8]. Generally, polymer flooding enhances the sweep

efficiency by three major mechanisms, including increasing the viscosity of the water/brine, minimizing water/brine permeability through swept areas, and covering a larger volume of the reservoir [3]. Polymer flooding typically does not generally increase the microscopic displacement efficiency of light oils, though recent studies strongly suggest that viscoelastic polymeric solution may be able to improve the microscopic displacement efficiency relative to waterflood [9]. In practice, two commercial polymers, partially hydrolyzed polyacrylamides (HPAM) and xanthan gums, are commonly used in oil field enhanced oil recovery (CEOR) applications. HPAM is a water-soluble polyelectrolyte with negative charges on the polymer chains. Xanthan gums, which are polysaccharides, show excellent viscosifying ability and high tolerance to salinity but degrade with an increase in temperature and are sensitive to biodegradation [10]. Additionally, clay (bentonite) of smectite groups is being utilized in different oil field applications as well, especially in drilling fluids technology as a rheology enhancer. Recently, Abdelhady [11] reported that the efficiency of HPAM-based polymer flooding was enhanced with the addition of clay due to its superior rheological property. Still, the widely employed HPAM and PAM polymers suffer hydrolysis and degradation under high temperature, mechanical stress, and salinity conditions [12–16]. Polymer molecular chains undergo scission, leading to a great reduction in the polymer viscosity [17,18]. Hence, a high concentration of polymer is utilized, which incurs huge additional cost [19]. In addition, the reservoir heterogeneity leads to extraneous water channeling from different layers to the oil swept zone and also polymer loss to the adjacent zone [2].

The application of nanotechnology in the petroleum industry has evolved significantly over the past decade. Nevertheless, the use of NPs in CEOR field application is very limited. The advantages of combining polymer flooding with NPs, i.e., nanohybrid, including rheology enhancement, salt tolerance, thermal stability, shear tolerance, and other rock–fluid/fluid–fluid interactions [3]. Still, results suggest that some nanohybrids, e.g., SiO_2/HPAM, suffer from reduced viscosity with an increasing temperature and salt concentration due to thermal degradation and the accumulation of the sodium cations onto the amide group, which leads to shrinkage of the polymer chains and the minimization of crosslinking [16,20]. Metallic NPs have been used extensively in the development of HPAM water-based drilling fluids [21,22]. Nevertheless, limited studies have addressed metallic oxide NP's performance for CEOR applications [23]. Shah [24] performed laboratory CEOR experiments using CuO NPs for oil with an API gravity of 15 in a Berea sandstone core. The rheological properties improved and 1 wt.% CuO NP achieved a 71% oil recovery by virtue of the enhanced hydrophilic characteristics of the nanofluid [25]. It was suggested that if the electronegativity difference between the metal and the oxygen atoms is in between 0.5 and 1.7, the metal oxide is considered polar or hydrophilic, and if the electronegativity difference is < 0.5, the metal oxide is considered non-polar or hydrophobic [25]. For CuO, the electronegativity difference is 1.5 [26]; hence, cupric oxide is hydrophilic and effectively disperses in water. The addition of CuO to a polymer solution should, in principle, enhance the temperature and the salt tolerance, as confirmed by published studies [21,22,24].

Another issue relating to HPAM polymer flooding is the tendency of the polymer for adsorption onto the formation. Although adsorption of the polymer may mitigate reservoir heterogeneity and act as a conformance control agent, polymer retention leads to a reduction in fluid viscosity, irreversibly reservoir damage [27], and loss of polymer. It is noted that, depending on the size of polymer molecules, their aggregation state, and the rheology of the polymer solution, some polymer molecules are trapped, rather than adsorbed, within reservoir pores. Adsorption of polymer molecules onto NPs, or vice versa, may mitigate the risk of polymer molecules' retention [3]. Nanoclay, on the other hand, aids in proper plugging of undesired channels, i.e., profile modification, and helps to maintain proper polymer rheology owing to its effective interaction with HPAM molecules [20,28]. Additionally, nanoclay works as a filler in the polymer matrix to enhance its mechanical strength. Recently, Tiwari and their group [29] reported that nanoclay can be used as a loss circulation agent for drilling fluids and can enhance the rheology without increasing the weight of the fluid. Kumar et al. [23] developed a novel grafted copolymer onto clay/CuO and explored its application in drilling shale wells under harsh reservoir conditions. Thus, formulating a nanohybrid system consisting of nanoclay in addition

to CuO and HPAM polymer can be a better alternative to overcome reservoir heterogeneity and a harsh environment.

In the current study, nanohybrid systems comprising of a blend of nanoclay and CuO NPs together with HPAM polymer were tested with the objective of improving the rheological properties of HPAM as well as its thermal and salt tolerance. The preparation steps of the nanohybrid are convenient and not too exhaustive, which promotes the field applicability of the system. Control samples consisting of HPAM were tested in the same conditions in order to isolate the role of the nano-additives. Furthermore, oil recovery tests were carried out in sandpacks at 85 °C and a salt concentration of 1 wt.% and a comparison between the nanohybrid performance and HPAM was made.

2. Experimental Methods

2.1. Materials

Laboratory-grade potassium chloride (KCl) and distilled water was procured from the Department of Petroleum and Energy Studies, Dehradun Institute of Technology University (DIT University, Dehradun, Uttarakhand, India). Partially hydrolyzed polyacrylamide (HPAM) was obtained in a dry form from Oil and Natural Gas Corporation (ONGC, Dehradun, Uttarakhand, India). Nanoclay ($\bar{d}_p$ < 25 nm) and CuO NPs ($\bar{d}_p$ < 50 nm) of synthesis grade were purchased from Sigma Aldrich (Mumbai, Maharashtra, India). Silica sand of a mesh size 100–140 was procured from ONGC (Dehradun, Uttarakhand, India). Synthetic oil of 226 cP (at 85 °C) was procured from Chevron Philips Company (Texas, USA).

2.2. Properties of the Sandpack

The initial porosity of the sandpack was measured using the gravity saturation method [30]. The absolute permeability was estimated by injecting a brine into the sandpack from the top at 25 °C and correlating the flow rate and pressure drop across the sandpack [30]. The brine solution was prepared by mixing deionized (DI) water and 1.1 wt.% KCl. The synthetic oil was filtered upon receiving it and its density and viscosity at 23 °C were 0.89 g/mL and 1190 cP, respectively. Table 1 summarizes the properties of the sandpack and the packing material.

Table 1. Properties of the cylindrical sandpack and the packing material at ambient conditions.

Properties	Values
Length (cm)	30.48
Cross sectional area (cm^2)	16.79
Density of sand (g/mL)	2.45
Porosity (%)	33.4 ± 3
Absolute permeability (Darcy)	5.0 ± 1.4

2.3. Preparation of the Different Fluid Systems

Different masses of CuO NPs (0.1–0.5 g) and nanoclay (0.3–0.6 g) were mixed in 50 mL of DI water followed by sonication for 8 h at 60 °C to produce a stable dispersion. The higher temperature during sonication enables easier dispersion of the NPs. The brine solution was prepared by mixing 5.0 g KCl in 500 mL of distilled water using a magnetic stirrer. A mass of 2.5 g of HPAM was added to the 500 mL of brine solution and stirred for 16 h to obtained a 0.5 wt.% stable polymer solution, which was used as a control sample. Nanohybrid systems 1 to 8 were prepared by adding the 50-mL water dispersion containing different masses of CuO NPs and nanoclays to 450 mL of the HPAM brine solution. Table 2 lists the composition of the different fluid systems employed in this study.

Table 2. Composition of the polymer solution (control) and the nanohybrid systems used in this work.

Constituents	Control	Nanohybrid 1	Nanohybrid 2	Nanohybrid 3	Nanohybrid 4	Nanohybrid 5	Nanohybrid 6	Nanohybrid 7	Nanohybrid 8
DI water (mL)	500	500	500	500	500	500	500	500	500
HPAM (g)	2.5	2.5	2.5	2.5	2.5	2.5	2.5	2.5	2.5
KCl (g)	5.0	5.0	5.0	5.0	5.0	5.0	5.0	5.0	5.0
Nanoclay (g)	–	0.5	0.5	0.5	0.5	0.5	0.3	0.4	0.6
CuO NPs (g)	–	0.2	0.1	0.3	0.4	0.5	0.2	0.2	0.2

2.4. Analysis

The surface morphology of the CuO NPs, nanoclay, HPAM control, and nanohybrid 1 was analyzed using scanning electron microscopy (SEM, Jeol JSM 5910 LV, Jeol India pvt. Ltd., New Delhi, India) operated at 220 V, 110 AC, 30 A, and 3kV total load. Initially, all reagents were conditioned in a vacuum oven at 65 °C for 16 h to reduce their moisture content [29]. Then, the reagents were coated with platinum prior to SEM analysis to mitigate the potential charge effect due to moisture and increase the reliability of the measurements [3]. Platinum coating was used since it reduces the required coating thickness by half relative to the commonly used gold coating. The thinner coating better reveals the fine microstructure and is less affected by the temperature and substrate composition [23].

The rheological properties of the HPAM polymer control solution and the nanohybrid systems were evaluated by measuring the apparent viscosity using an Anton Paar rheometer (Anton Paar Analytical Instrument Company, Ashland, Virginia, USA) at 85 °C. This temperature is a frequently encountered reservoir temperature during polymer flooding [31]. The flow models of the HPAM polymer solution and the nanohybrid systems were extracted from the relationship between the shear stress and the shear rate as well as the viscosity vs. shear rate in a cartesian coordinate system at shear rates ranging from 10 s^{-1}–100 s^{-1} [32]. Both, the polymer solution and the nanohybrid systems, were initially hot rolled in an oven at 70 °C for 10 h prior to the rheometer measurements. The thermal degradation behavior of the nanohybrid system was assessed using thermogravimetry analysis (TGA, Netzsch-STA 449, Jupiter bench model, Fukuoka, Japan) of a dried droplet of nanohybrid 1. The dried sample of the HPAM polymer solution was used as the control sample. The TGA test was conducted for a temperature ranging between 150 and 500 °C with a heating rate of 23.7 °C/min under an N_2 atmosphere. In addition, the thermal stability of the polymer solution and nanohybrid 1 system was analyzed using an electrically driven hot roller oven (Fann Instrument Company, Texas, USA) equipped with an aging cell. The dynamic aging test was used following a detailed procedure published earlier by our group [33]. In brief, the samples were introduced to the hot roller cell. The temperature of the oven was varied from 23 to 130 °C and the thermal stability was analyzed by measuring the apparent viscosity of the aged HPAM polymer solution and the nanohybrid 1 system and comparing it with their freshly prepared samples. All the above-mentioned tests were replicated twice to ensure the reproducibility of the results.

The salt tolerance of the polymer solution and nanohybrid 1 system was determined by varying the KCl concentration in the brine solution used to prepare the polymer and the nanohybrid from 2.5 to 12.5 g. All samples were aged in the hot roller oven at 70 °C for 10 h prior to measuring their apparent viscosity and consistency following procedures recommended by the American Petroleum Institute [9,33]. A comparison between the values of consistency and apparent viscosity for the samples at different salt concentrations was used to draw conclusions on salt tolerance.

The core flooding analysis in the sandpack was carried out to assess the oil recovery potential of the polymer solution and nanohybrid 1 and compare it with the brine injection as a representative of water flooding. The flooding experiments were conducted at 2413.2 kPa injection pressure and 5481.3 kPa overburden pressure at 85 °C. The overburden pressure was imposed hydraulically using stainless-steel-made confining sleeve sets inside the center of the sandpack, and the hydraulic pressure inside the confining sleeve was maintained using a nitrogen cylinder connected to it. First, 2.5 pore volume (PV) of the 1.1 wt.% KCl brine solution was pumped into the sandpack to mimic connate water. Then, the synthetic oil injection commenced into the sandpack and continued for 2 PV to achieve the irreducible water saturation (S_{wir}). The mass balance was used to estimate water saturation. Nanohybrid 1, HPAM polymer (control) solution, or brine was injected for 1 PV at a rate of 1 mL/min to displace the oil. The experiments were replicated at least two times to ensure reproducibility. The recovery factor (*RF*) was calculated using Equation (1) [4]:

$$RF = \frac{S_{oi} - S_{or}}{S_{oi}} \times 100\% \quad (1)$$

where S_{oi} is the initial oil saturation and S_{or} is the residual oil saturation following flooding. A schematic of the sand pack flooding setup is given in Figure 1.

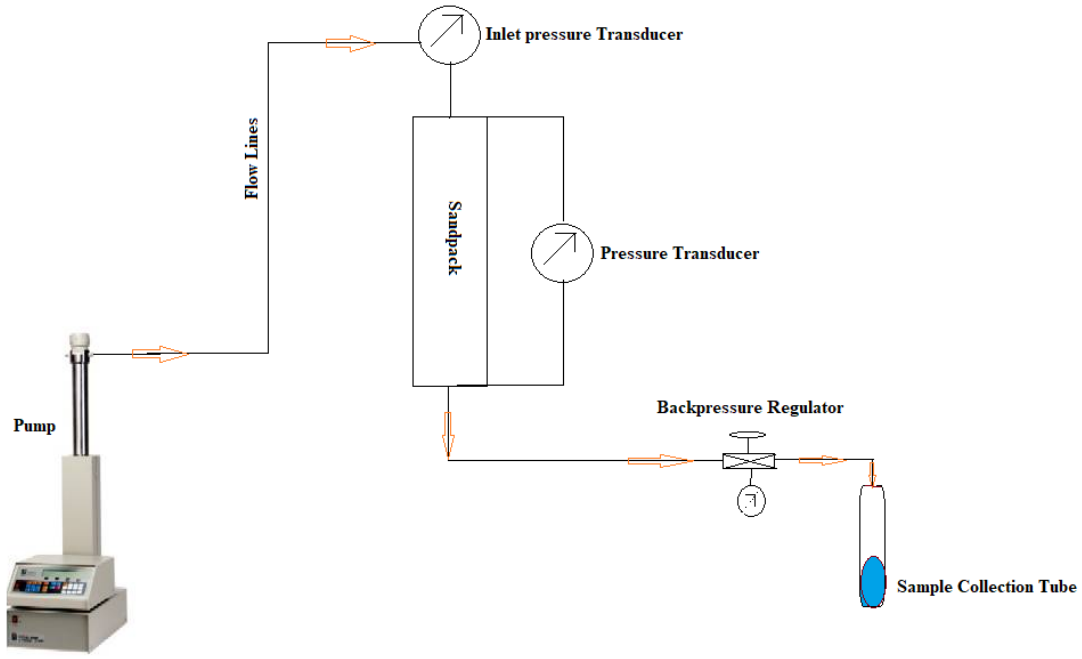

Figure 1. Schematic of the sandpack flooding setup.

3. Results and Discussions

3.1. SEM Analysis

The surface morphology of the CuO NPs, nanoclay, HPAM solution, and nanohybrid 1 were examined by SEM, as shown in Figure 2. It is noted that nanohybrid 1 and the HPAM polymer solution were left to dry before SEM images could be taken. Figure 2a shows that CuO NPs are agglomerated and display irregular clusters with some crystalline structure, whereas a smooth regular and spongy surface is displayed by the nanoclay, as evident from Figure 2b. The surface morphology of HPAM polymer (Figure 2c) was altered by the addition of CuO NPs and nanoclay and well-distributed pockets of agglomerates appeared (Figure 2d). Figure 2d suggests that nanoclay was dispersed in the HPAM matrix [28], likely together with the CuO NPs. At this level of dispersion, the interaction among CuO NPs, nanoclays, and the polymer gives rise to a network structure, which favorably affects the rheological properties of the nanohybrid flooding fluid [3,21].

3.2. Thermogravimetric Analysis

TGA profiles of the dried nanohybrid 1 system and HPAM solution are included in Figure 3. Both the HPAM and nanohybrid 1 show one major mass loss step. The small initial loss observed between 150 and 200 °C, 0.12 g for nanohybrid 1 and 0.60 g for HPAM solution, is attributed to the evaporation of remaining moisture associated with the samples [34,35]. Considering the dried HPAM solution, two major mass loss zones appear for T > 200 °C. The first zone, 200–320 °C, corresponds to the loss of 5.43 g of thermally degraded polymer chains, which evaporated at the high temperatures. In the meantime, the remaining longer chains undergo polymerization, which was partly degraded under the higher temperatures of the second zone, 320–500 °C. The remaining 2.3 g at T = 500 °C correspond to a highly polymerized/coked product. Two zones also appear for T > 200 °C for the

dried nanohybrid 1 TGA profile. The first zone, 200–310 °C, which corresponds to the loss of 4.55 g for nanohybrid 1, was attributed to the evaporation of short-chain scission products. The second zone, 310–500 °C, corresponds to 0.9 g of thermally degraded longer polymer chains. The 4.5 g remaining at T = 500 °C correspond to 0.5 g of nanoclay, 0.2 g of CuO NPs, and 3.8 g of highly polymerized polymer/coke product. Given the mass percent of the HPAM in nanohybrid 1, i.e., 78 wt.%, one may conclude that a similar amount of the polymer was lost in the first zone for both HPAM and nanohybrid 1, whereas a much lower loss of the HPAM was experienced at higher T in the presence of the NP additives. This suggests that the CuO NPs and the nanoclay provided thermal stability to the polymer chains, likely through adsorption of the polymer radicals onto the NPs.

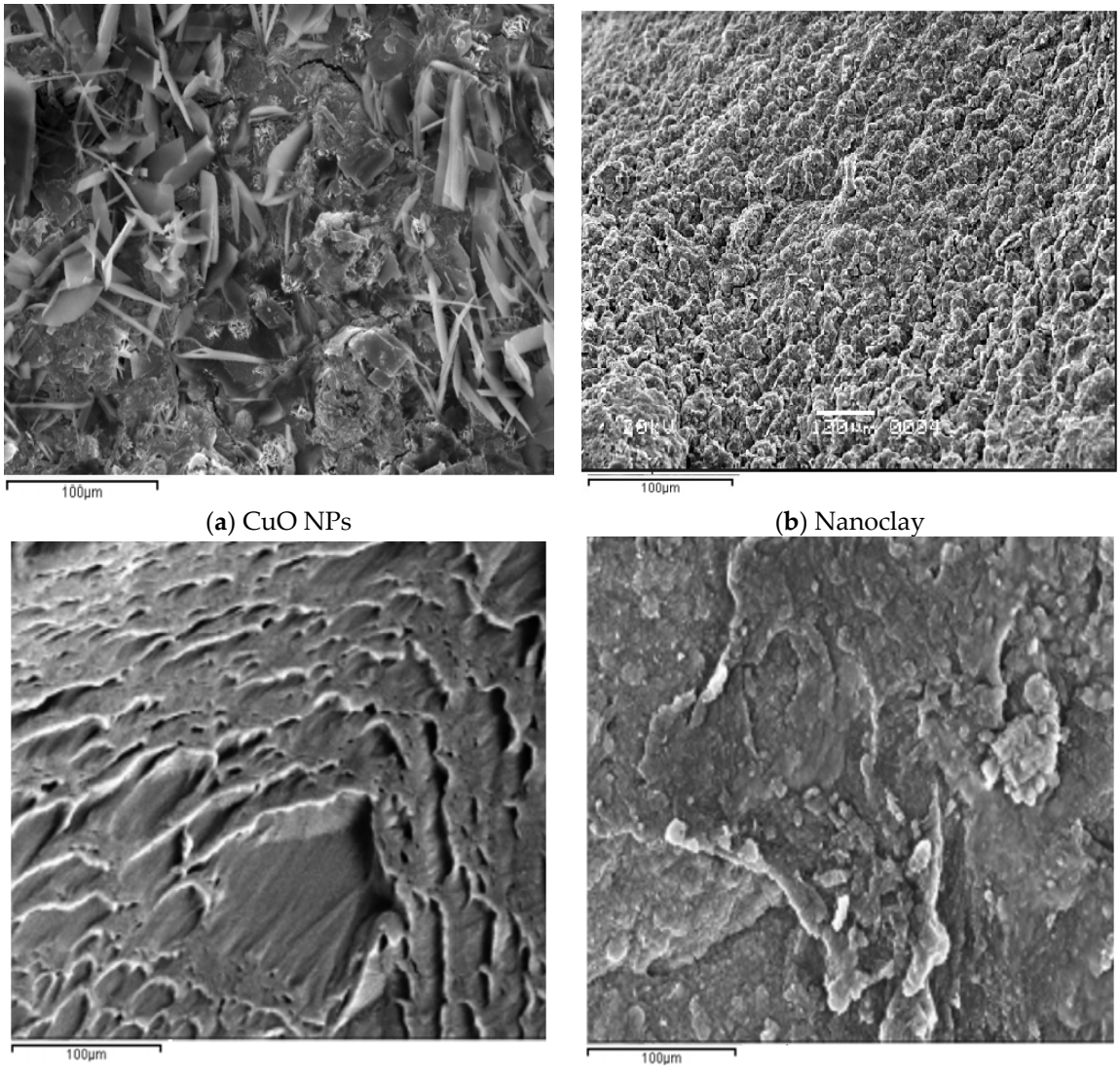

(**a**) CuO NPs (**b**) Nanoclay

(**c**) HPAM (**d**) Nanohybrid 1

Figure 2. SEM images of (**a**) CuO NPs (nanoparticles); (**b**) nanoclay; (**c**) dried HPAM (Partially hydrolyzed polyacrylamide) solution; and (**d**) dried nanohybrid 1.

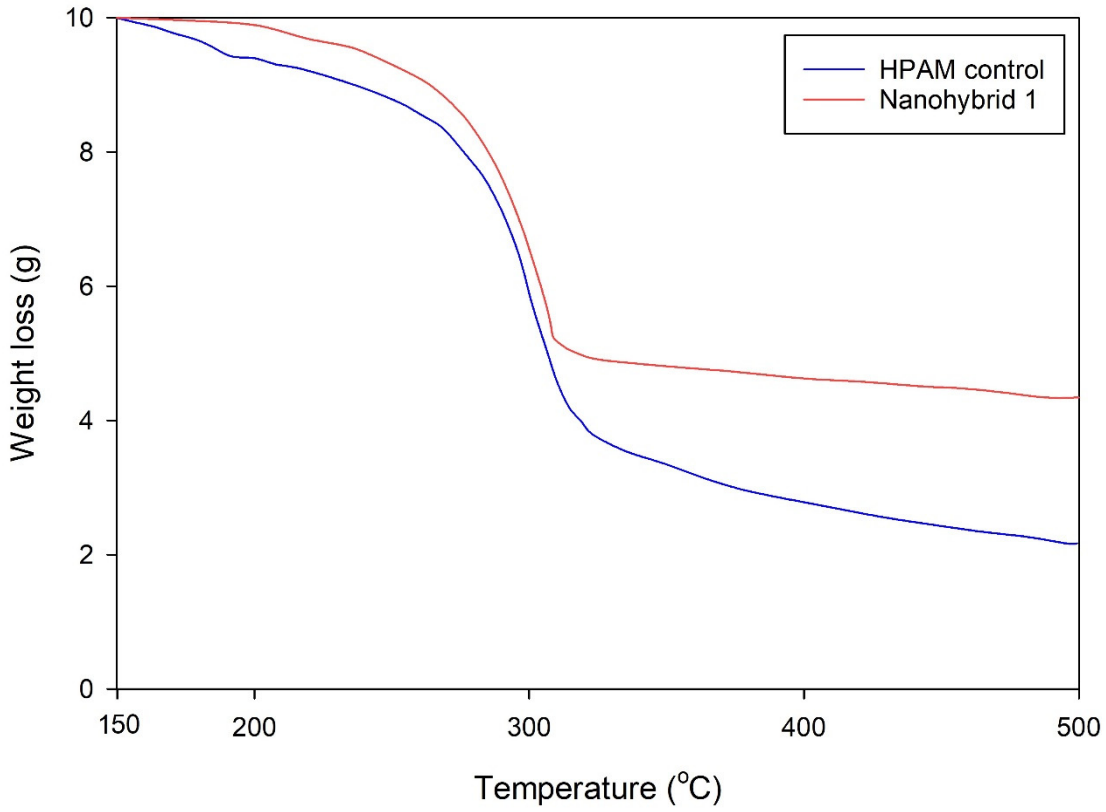

Figure 3. TGA (thermogravimetric analysis) profile of dried samples of HPAM (Partially hydrolyzed polyacrylamide) solution and nanohybrid 1.

3.3. Rheological Behavior of the HPAM Solution and the Nanohybrid Systems

The apparent viscosity of the HPAM solution and nanohybrid systems 1–8, with different compositions of CuO NP and nanoclay, are reported in Figure 4. The CuO NP content was varied in the nanohybrid systems 1 to 5 from 0.1–0.5 g at a constant content of nanoclay of 0.5 g, while the nanoclay content was varied in the nanohybrid systems 6 to 8 from 0.3–0.6 g at a constant CuO NPs of 0.2 g.

Figure 4 shows that increasing the content of CuO NPs and the nanoclay increased the viscosity of the HPAM solution significantly. This increase in viscosity is attributed to the effective dispersion of the nanoclay in the HPAM polymer matrix owing to hydrogen bonding between HPAM and the nanoclay [28,36,37], the network structure of the nanohybrid [3], and the adsorption of CuO NPs onto the HPAM (and vice versa) [21], as evident from Figure 2d. Gou et al. [28] reported that hydrogen bonds are established between charged oxygen and hydroxyl groups of the nanoclay with the carbonyl group of HPAM. It is worth mentioning that nanohybrid 2 and 6 have a lesser concentration of CuO NPs (0.1 g) and nanoclay (0.3 g), which results in a lower viscosity than the other nanohybrid systems, but still higher than that of the HPAM control sample. It is noted that nanohybrid 1 displayed acceptable viscosity, i.e., < 200 cP [38], which ensures a proper mobility ratio while decreasing the pumping cost and avoiding injectivity issues [39]. Thereby, nanohybrid 1 appears to be the best candidate for potential CCEOR applications [38].

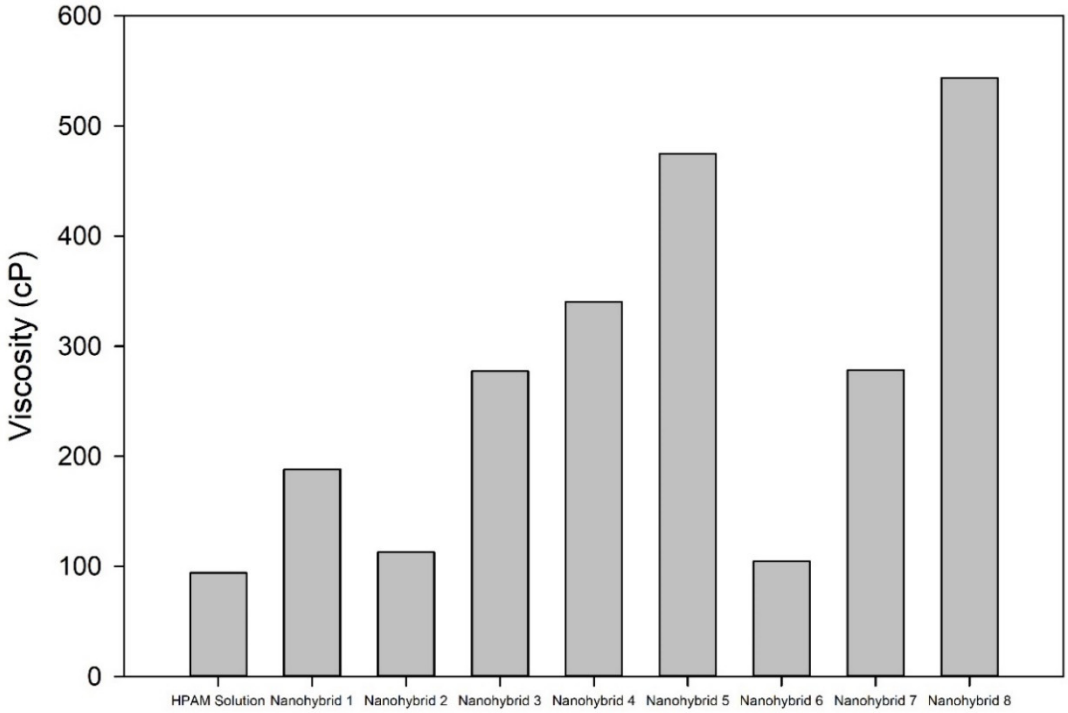

Figure 4. Apparent viscosity of HPAM solution and nanohybrid systems as per Table 1. Shear rate = 10 s^{-1}, T = 85 °C.

The HPAM polymer solution and the nanohybrid systems were aged for 10 h at 85 °C and their apparent viscosity at a varying shear rate (10–100 s^{-1}) was reported. For a given shear rate, these viscosities were recorded after 15 min. Figure 5 shows that the viscosity decreases with an increasing shear rate for all the fluid systems, which suggests a pseudoplastic (or shear thinning) behavior [29]. The decrease in viscosity with an increasing shear rate may result from the shear degradation of the HPAM molecules [18,33] and/or from disentanglement and alignment of the polymer chains along the direction of shear. Except for nanohybrid systems 2 and 6, which had a lower content of CuO NPs and nanoclay, as explained earlier, all nanohybrid systems displayed higher viscosities than HPAM solution for all the different shear rates. Accordingly, nanohybrid systems portray superior shear resistance properties compared with HPAM polymer solution [33,40]. It appears that the strong initial dispersion of the nanoclay in the HPAM solution, by virtue of hydrogen bonding, reduced the extent of polymer chain degradation [12] and maintained a higher extent of entanglement among the polymer chains at the higher shear rate. Moreover, the adsorption of CuO NPs onto the polymer strengthens the entanglement among the polymer chains, which reduces the shear sensitivity of the polymer [23]. It is noted that during polymer flooding, the polymer molecules are subjected to high levels of shearing, especially at the exit of the injector well [3,12]. Hence, a shear thinning behavior is desirable, since it reduces the extent of momentum loss due to friction.

The relationship between the apparent viscosity and shear rate was reproduced after keeping the nanohybrid systems and the polymer solution standing (aging) for 15 h at 85 °C and remeasuring the viscosity in the dynamic condition (shear rate = 10–100 s^{-1}). Figure 5 confirms that almost all the nanohybrid systems retained their original viscosity, as opposed to the HPAM polymer solution. Retaining the same viscosity suggests that the nanohybrid systems exhibit a viscoelastic property, in addition to their pseudoplastic behavior. For example, nanohybrid 1 retained its viscosity at every shear rate, which suggests strong viscoelastic behavior. The HPAM polymer solution did not retain its initial viscosity, even at a low shear rate, likely due to mechanical degradation of the polymer chains at a high shear rate [41–43]. The remarkable performance of the nanohybrid systems could be attributed to the hydrogen bonding of HPAM with the nanoclays as well as the strong adsorption of the CuO

onto HPAM, or vice versa [29,41], which strengthens the HPAM polymer network. Such an interaction among the polymer and the NPs preserved the polymer chains from degradation and maintained a high extent of entanglement among the polymer chains attached to the NPs even under shearing.

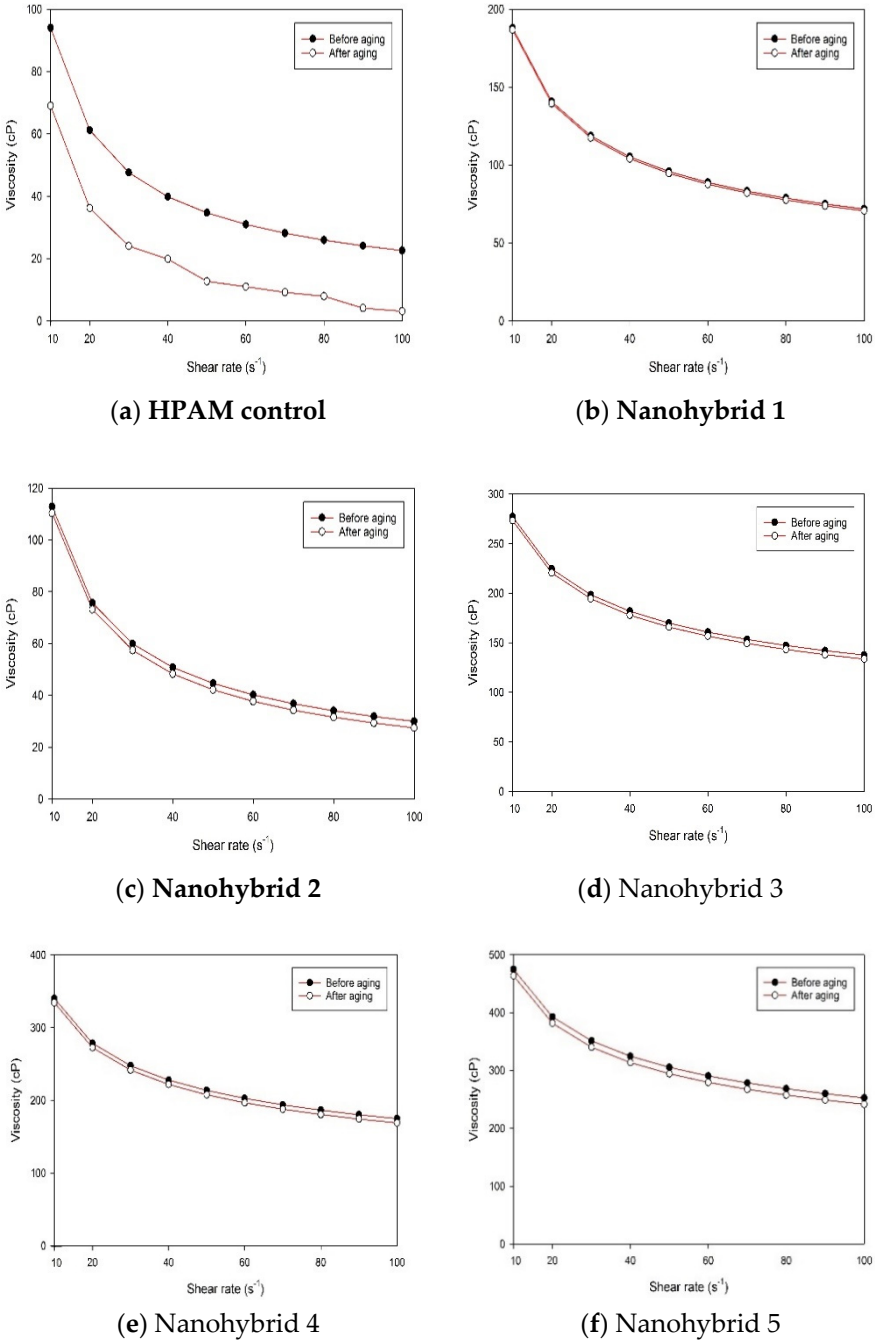

(**a**) **HPAM control** (**b**) **Nanohybrid 1**

(**c**) **Nanohybrid 2** (**d**) Nanohybrid 3

(**e**) Nanohybrid 4 (**f**) Nanohybrid 5

Figure 5. *Cont.*

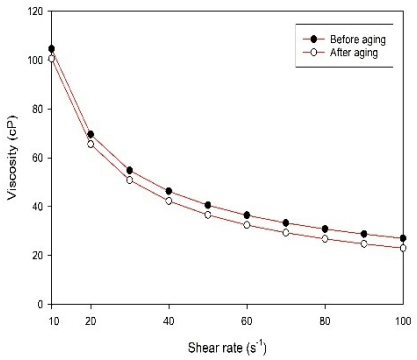

(**g**) Nanohybrid 6

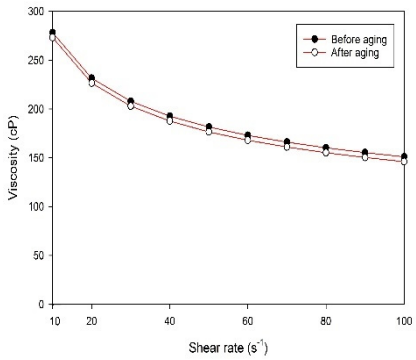

(**h**) Nanohybrid 7

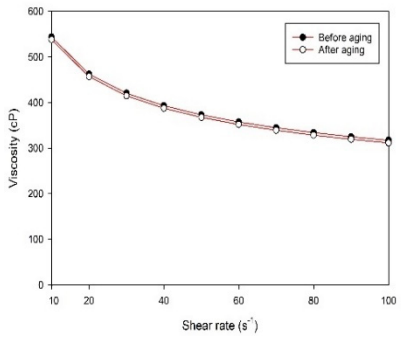

(**i**) Nanohybrid 8

Figure 5. Apparent viscosity vs. shear rate of HPAM polymer solution and nanohybrid systems 1 to 8. T = 85 °C.

To demonstrate the effectiveness of the nanohybrid 1 system formulated in this work, a comparison was made with the work of Cheraghian and Nezhad [44], who formulated HPAM/nanoclay nanohybrid for CEOR application. A plot of the apparent viscosity vs. shear rate is given in Figure 6 (at room condition for Cheraghian and Nezhad [44]) and nanohybrid 1 (current study). Despite the higher T used in our study (85 °C), further enhancement in the viscosity of the HPAM solution was achieved with the combined addition of nanoclay and CuO NPs. It is worth noting that higher viscosities during polymer flooding operations better suit heavier oil reservoirs.

The pseudoplastic behavior of the polymer solution and the nanohybrid systems can be represented by Equation (2) [21]:

$$\tau = \tau o + K\gamma^n, \quad (2)$$

where τ is the shear stress (Pa), τo is the yield stress (Pa), γ is the shear rate (s^{-1}), K is the consistency ($Pa{\cdot}s^n$), and n is the flow behavior index (dimensionless). Figure 7 is a log-log plot of τ vs. γ for the HPAM solution and the nanohybrid systems. The coefficient of determination, R^2, is > 0.96 for all the curves, as shown in Table 3, which also lists the values of K and n as obtained from the fit. Gou et al. [28] stated that only polymer fluid systems having n between 0.5 and 0.7 can retain their original viscosity at different shear conditions, i.e., possess strong viscoelastic characteristics. Accordingly, nanohybrid 1 shows strong viscoelastic behavior, i.e., entirely retained its original viscosity, and displayed a flow behavior index, n, of 0.582. HPAM polymer solution, on the other hand, did not retain its original viscosity and displayed a flow behavior index, n, of 0.38. Moreover, the flow behavior index, n, for nanohybrid systems 2–8 was close to the range given by Gou et al.; hence, these systems portrayed good viscoelastic behavior.

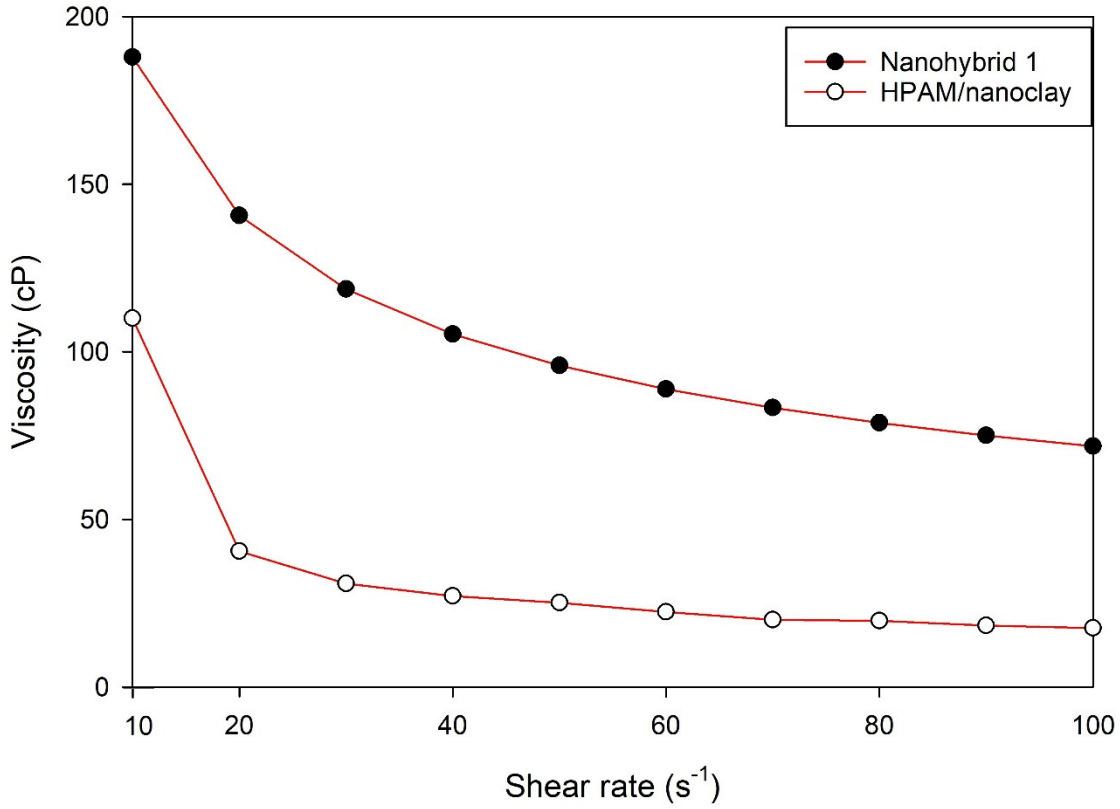

Figure 6. Comparison between the apparent viscosity of nanohybrid 1 (at 85 °C) with a nanoclay-based nanohybrid composed of 0.9 g of nanoclay and 3.2 g of HPAM (at T~ 25 °C) [44].

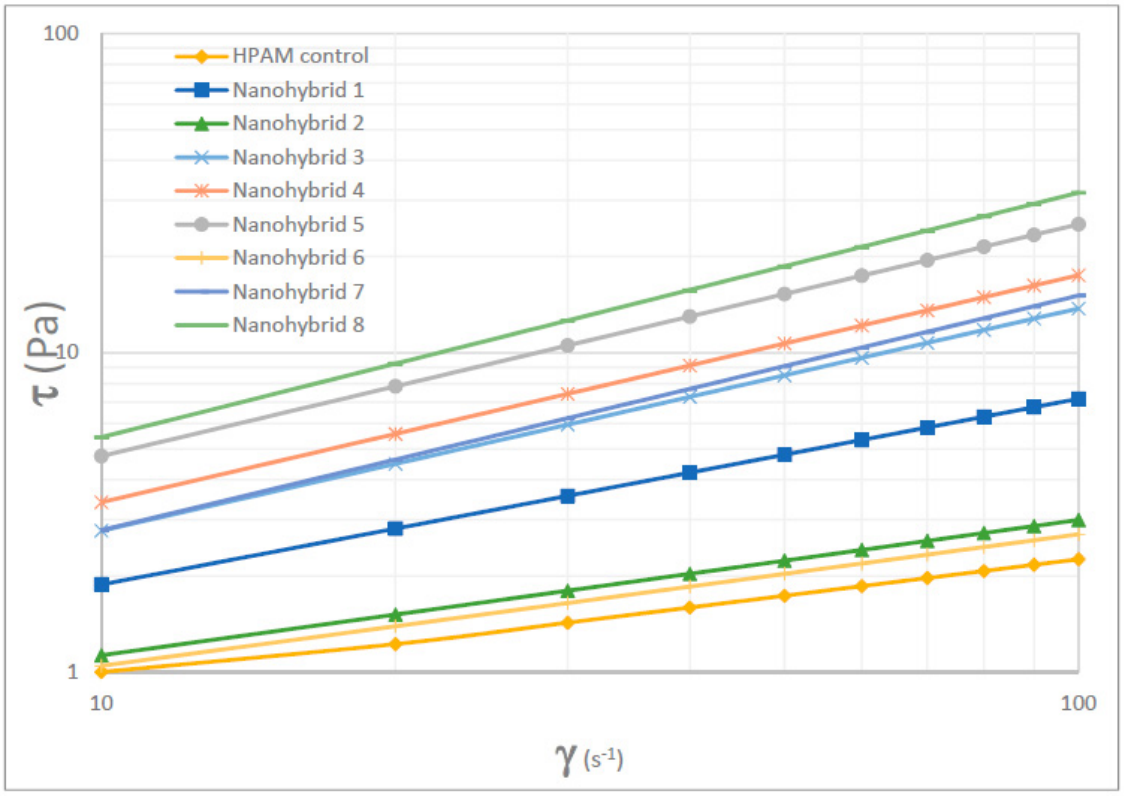

Figure 7. A plot of the shear stress vs. shear rate curve for the formulated nanohybrid compositions and HPAM polymer solution. T = 85 °C.

Table 3. Hershel–Bulkley law coefficients and coefficient of determination, R^2, values for the HPAM polymer solution and the nanohybrid systems.

Fluid Systems	K	n	R^2
HPAM control	0.392	0.38	0.9625
Nanohybrid 1	0.492	0.582	0.9998
Nanohybrid 2	0.425	0.424	0.9899
Nanohybrid 3	0.558	0.702	0.9789
Nanohybrid 4	0.662	0.711	0.9822
Nanohybrid 5	0.892	0.726	0.9625
Nanohybrid 6	0.405	0.412	0.9825
Nanohybrid 7	0.512	0.735	0.9648
Nanohybrid 8	0.932	0.766	0.9648

3.4. Thermal Stability of the Polymer Solution and Nanohybrid 1

The effect of temperature on the apparent viscosity of HPAM polymer solution and nanohybrid 1 is reported in Figure 8. The temperature effect is negligible on nanohybrid 1, whereas appreciable on HPAM polymer solution, especially for T > 80 °C. The apparent viscosity of the HPAM polymer solution dropped from ~100 to ~10 cP upon changing the temperature from 80 to 100 °C. For nanohybrid 1, viscosity only decreased from 190 to 160 cP with T increasing from 23 to 130 °C. Temperature degrades both the intermolecular and the intramolecular interactions among and within the HPAM polymer molecules [9]. On the other hand, the increased adsorption/interaction of HPAM onto/with CuO NPs in nanohybrid 1 at the higher temperature protected the polymer from degradation and increased the stability of the colloidal system [45], likely through steric hindrance. At T > 100 °C, a slight decrease in the nanohybrid 1 viscosity was observed, likely following the general rule of temperature effect on the viscosity of liquids [29,41]. Overall, nanohybrid 1 is well suited for high-temperature oil reservoir CCEOR applications.

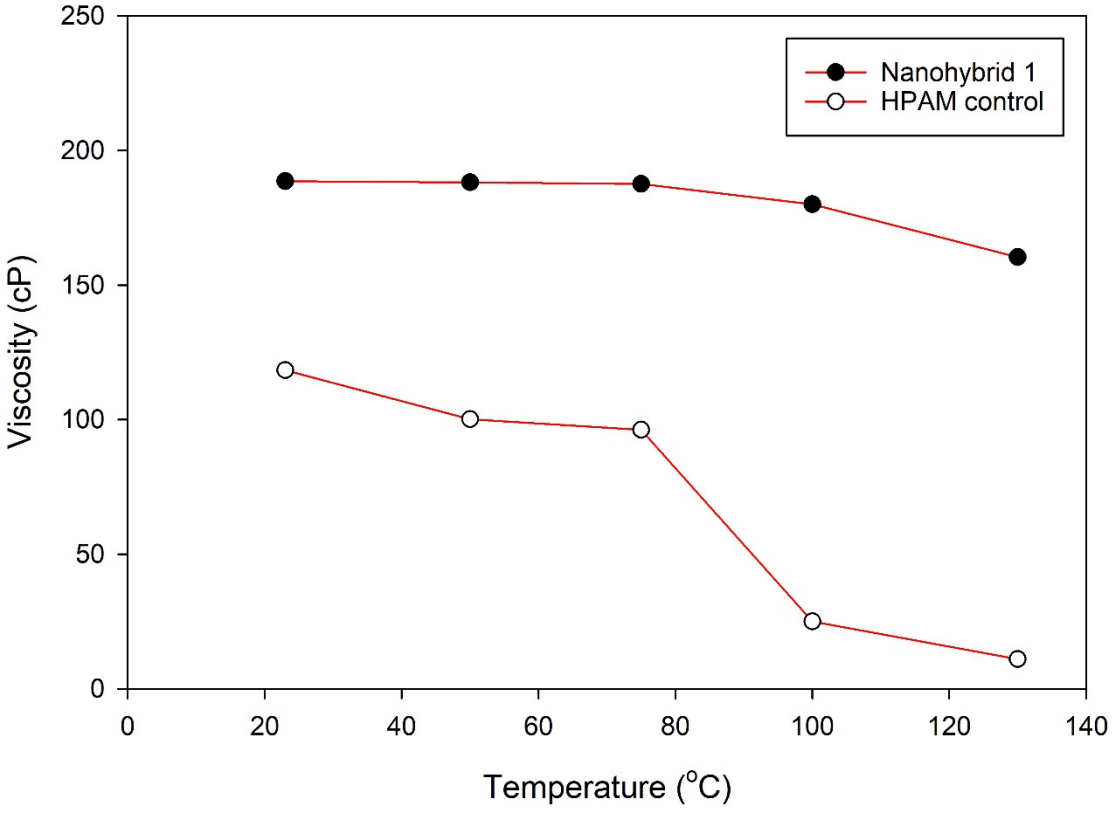

Figure 8. Temperature effect on nanohybrid 1 and HPAM polymer solution. Shear rate = 10 s^{-1}.

3.5. Effect Salinity

The concentration of KCl was varied from 5 to 12.5 g in the HPAM polymer solution and nanohybrid 1. The viscosities of these systems were measured at 85 °C and 10 s^{-1}, and the results are plotted in Figure 9. The viscosity of the HPAM polymer solution significantly decreased with the increasing salt concentration, dropping from 94 to 18 cP. It is noted that HPAM polymer molecules' interaction with the rest of the solution decreases at high ionic strength as the thickness of the hydration layer surrounding the ionic groups is compressed and the polymer molecules fold onto themselves, i.e., less entanglement of the polymer chains. The shrinkage of the electrical double layer also compromises the colloidal stability of the polymer solution. Conversely, the viscosity of nanohybrid 1 was constant, independent of the salt concentration. It is highly likely that at higher ionic strength, adsorption of the HPAM polymer onto the CuO NPs increases, which contributes to the stability of the colloidal dispersion via steric hindrance.

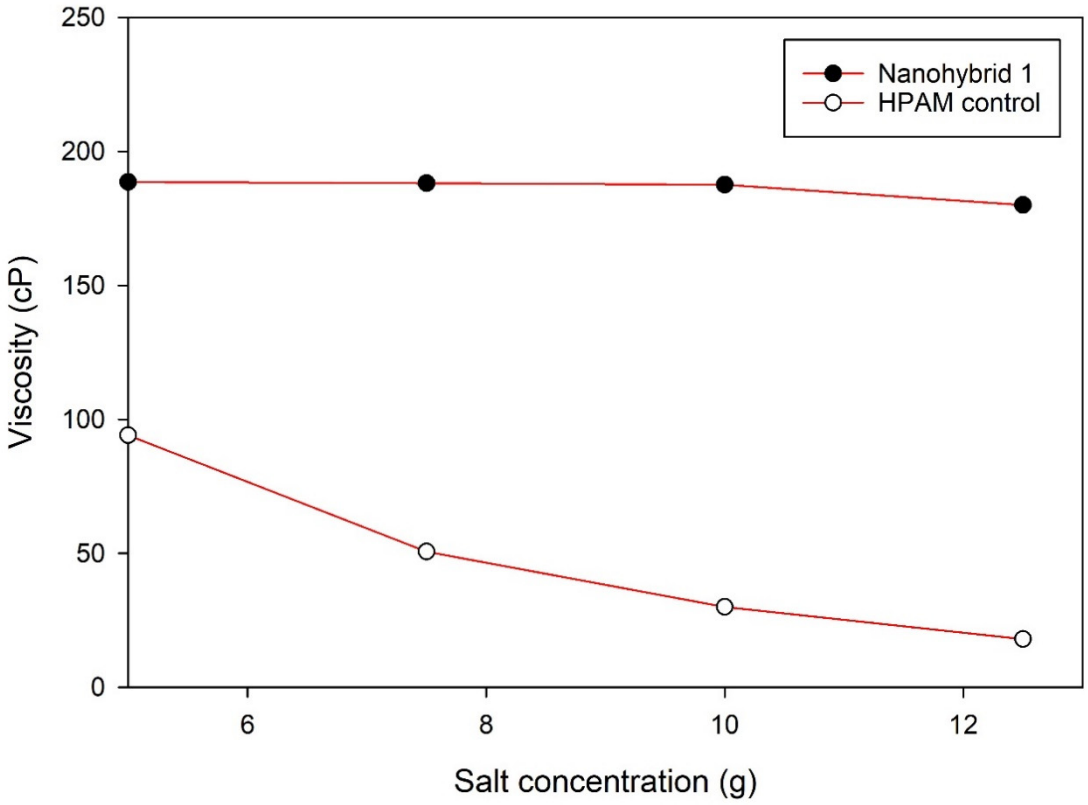

Figure 9. Effect of the salt concentration on nanohybrid 1 and HPAM polymer solution. Shear rate = 10 s^{-1}, T = 85 °C.

3.6. Displacement Tests

Displacement tests involved injecting brine solution, HPAM polymer solution, and nanohybrid 1 into the sandpack. Effective core flooding relies on the capillary end effect and potential viscous fingering, which is generally encountered due to a difference in the viscosity of the displaced and displacing phases. The capillary end effect generally arises due to the accumulation of the wetting phase at the outlet of the porous medium, which interrupts the breakthrough time. Rappaport and Leas [46] proposed a scaling coefficient to determine the effect of the capillary end inside porous media during a linear displacement process, as given below:

$$I = L * \mu_d * v, \quad (3)$$

where I is the scaling coefficient (cm^2·cP/min), L is the length of the sandpack (cm), μ_d is the viscosity of the displacing phase (cP), and v is the velocity of the displacing phase, which was calculated as the ratio of the flow rate (cm^3/min) of the pump divided by the cross-section area (cm^2) of the sandpack. Rappaport and Leas [46] suggested that the fluid flow in the sandpack remains insensitive to the capillary end effect if the scaling coefficient, I, is < 3.5 cm^2·cP/min. The scaling coefficient for each test is listed in Table 4. The values of the scaling coefficient suggest no capillary end effect during both HPAM polymer flooding and nanohybrid 1 flooding. For brine injection, on the other hand, the capillary end effect is pronounced, I = 0.64 cm^2·cP/min.

Table 4. Stability criterion results for brine, HPAM polymer solution, and nanohybrid 1 flooding.

Fluid Systems	Scaling Coefficient (I) (cm^2·cP/min)	Mobility Ratio
HPAM polymer solution	170.67	1.37
Nanohybrid 1	339.53	0.133
Brine solution	0.64	55.032

The viscous fingering, on the other hand, was assessed by the mobility ratio, which was calculated as follows [47]:

$$M = \frac{\mu_o * k_{rde}}{\mu_d * k_{roe}}, \quad (4)$$

where M is the mobility ratio, μ_o and μ_d are the viscosities of the oil phase and the displacing phase, respectively (cP), and k_{roe} and k_{rde} are the end point relative permeabilities of the oil phase and the displacing phase, respectively (dimensionless). The end point relative permeability to oil (k_{roe} and the displacing phase (k_{rde}) were determined after saturating the sandpack, and at the end of the polymer or nanohybrid 1 flooding using the Darcy law. Generally, end point relative permeability to oil is calculated at irreducible water saturation (minimum saturation of water below and at which water cannot flow inside the porous media) [48]. In other words, no water production should be observed at the end of the oil flooding stage, i.e., pressure drop stabilizes in the sandpack at this stage.

The primary oil flooding of the fully brine-saturated sandpack was performed and a piston-like displacement was attained in the sandpack, as evident from Figure 10. The pressure drop inside the sandpacks during oil flooding to attain S_{wir} while preparing the sandpack is shown in Figure 10 for the three sandpacks. The pressure drops reached the steady values, thereby an accurate end point relative permeability to oil was calculated. The results of the mobility ratio calculations for the three flooding experiments are listed in Table 4. It is highly desirable to maintain the mobility ratio, $M < 1$, in order to reduce viscous fingering issues [4]. Based on both, the scaling coefficient and mobility ratio, nanohybrid 1 appears the most suited of the flooding agents. Thereby, a higher recovery of oil is expected upon injecting nanohybrid 1.

Oil recovery from the sandpack was compared among the brine solution, the HPAM polymer solution, and nanohybrid 1 at ~2413.2 kPa injection pressure and 85 °C. The oil recovery expressed as the recovery factor (RF) per E1, as a function of the displacing phase pore volume (PV) injected, is reported in Figure 11. The residual oil saturation at the end of the flooding experiments was calculated using the material balance, and is reported in Table 5. As evident from Figure 11, oil recovery is the highest for nanohybrid 1 at every PV of injected fluid. At the end of the flooding experiment, i.e., PV = 1, RF of 88%, 61%, and 47% were attained for nanohybrid 1, HPAM polymer, and brine solution, respectively. As detailed earlier, nanohybrid 1 displayed excellent shear and thermal stabilities, hence a remarkable rheological performance, as well as an acceptable mobility ratio and scaling index. All these properties contributed to a piston-like displacement, which is effective toward oil recovery. HPAM polymer solution, on the other hand, appears to have suffered shear and thermal degradation at 2413.2 KPa and 85 °C.

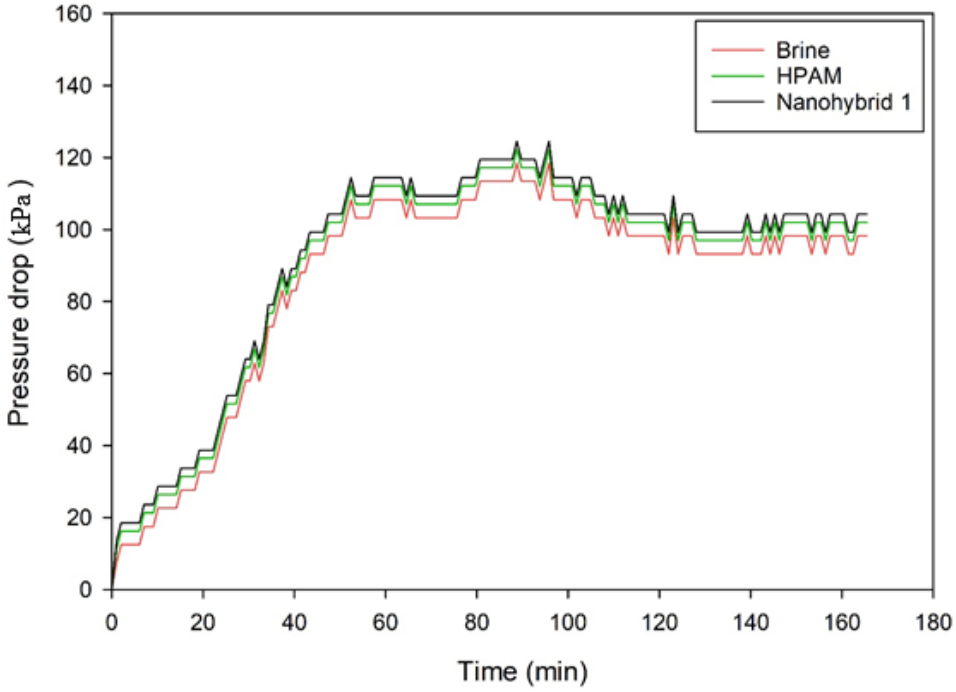

Figure 10. Pressure drop while saturating the sandpacks with oil during sandpack preparation. Shear rate = 10 s^{-1}, T = 85 °C.

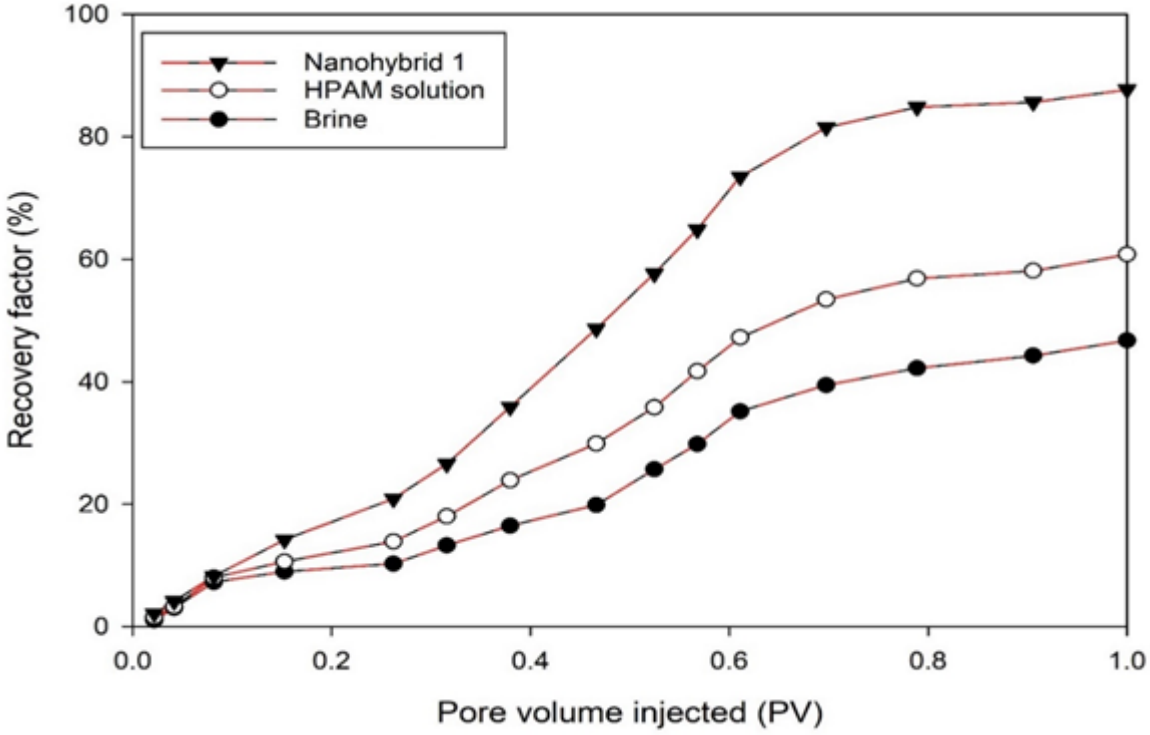

Figure 11. Oil recovery factor as a function of pore volume injection of nanohybrid 1, HPAM polymer, and brine solution.

Table 5. Properties of the sandpack and oil recovery parameters for different flooding experiments.

Fluid Systems	Permeability (mD)	Porosity (%)	RF (%)	Irreducible Water Saturation (Swir) (%)	Residual Oil Saturation (Sor) (%)
Brine solution	6318	36.8	46.75	9.58	48.15
HPAM polymer	5935	35.7	60.80	8.76	35.76
Nanohybrid 1	5014	33.4	87.74	8.12	11.26

The pressure drop in the sandpack during nanohybrid 1 flooding is plotted in Figure 12. The pressure drop for nanohybrid 1 injection suggests conformance control [3], entailing plugging high-permeability channels, and forcing the injected fluid into low-permeability zones. Table 5 summarizes the recovery factor, the irreducible water saturation, and irreducible oil saturation at the end of the different flooding experiments. The lower residual oil saturation confirms the efficacy of the nanohybrid 1 system in optimizing the oil recovery from the reservoir, including the conformance control attribute, under the experimental conditions.

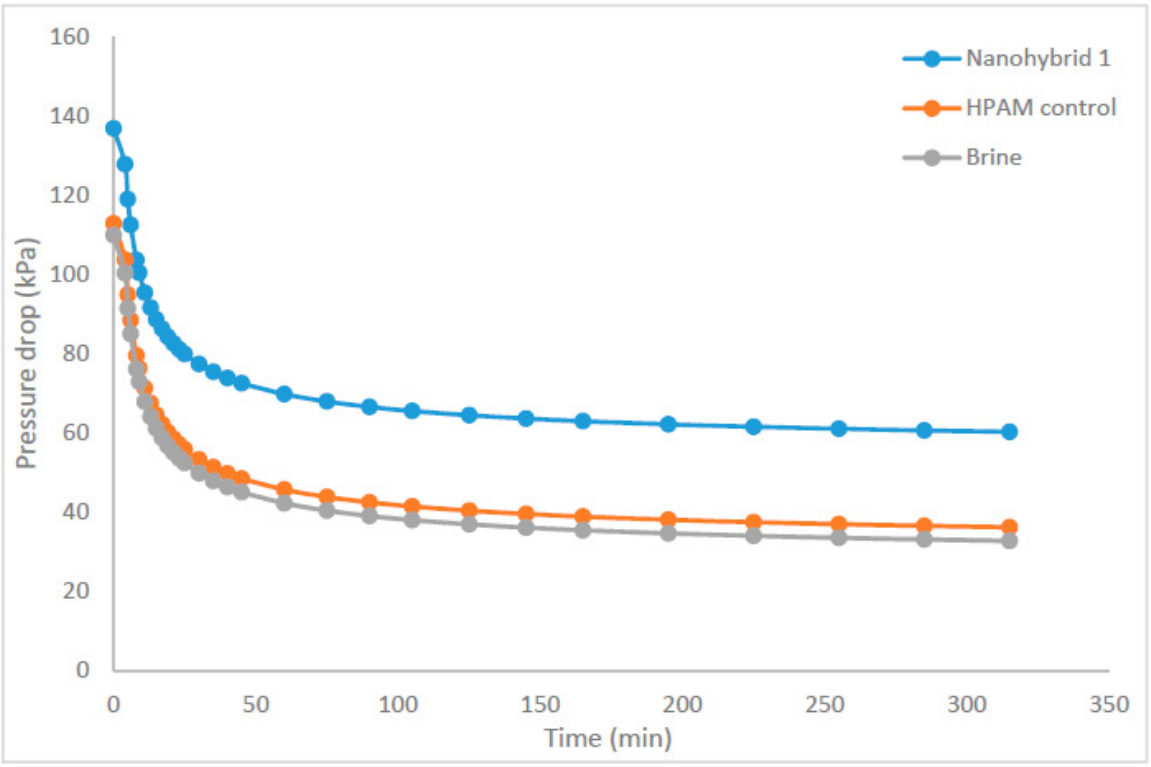

Figure 12. Pressure drop inside the sandpack during nanohybrid 1, HPAM, and brine flooding.

4. Conclusions

The rheological properties of a newly formulated nanohybrid composed of CuO NPs, nanoclay, and HPAM polymer were investigated under various conditions, including the additive content, salinity, temperature, and shear rate. Sandpack experiments were used to determine the recovery ratio among the nanohybrid system, HPAM polymer solution, and brine injection. The flooding tests were conducted in a linear sandpack at simulated reservoir conditions, i.e., ~2413.2 kPa of injection pressure and 85°C. Based on the analysis of the results, the following conclusions can be drawn:

SEM images of the nanohybrid suggests that the morphology of the HPAM surface was changed due to the adsorption of CuO NPs and dispersion of nanoclay in the HPAM matrix, which promoted the entanglement of the polymer chains even at high temperatures and salt concentrations.

Subsequently, the nanohybrid system maintained proper rheological properties, which in turn resulted in piston-like displacement of the oil and increased the recovery ratio/factor.

The rheological properties of the nanohybrid system depended on the content of the NPs (both CuO and nanoclay). Nanohybrid 1, consisting of 2.5 g of HPAM, 5 g of KCl, 0.5 g of nanoclay, and 0.2 g of CuO NPs in 500 mL of DI water, provided the most appropriate viscosity, which provides a suitable mobility ratio and scaling coefficient, while avoiding injectivity issues.

Combining CuO NPs and nanoclay helped to maintain higher viscosity at different shear rates, relative to the sole nanoclay additive or HPAM solution.

The combined effect of CuO NPs and nanoclay preserved the HPAM polymer from thermal and mechanical degradation and contributed to the superior viscoelastic property, in addition to the much desired pseudoplastic behavior.

The TGA results suggested that the nanohybrid system displayed remarkable temperature stability relative to HPAM polymer and potential applicability to a high-temperature reservoir without compromising the rheological properties of the flooding agent.

Author Contributions: S.K.: Conceptualization, Methodology, Investigation, Data curation, and Writing—Original Draft Preparation; R.T.: Methodology, investigation; M.H.: Supervision, Writing—Original draft preparation, Reviewing and Editing; N.K.: Project administration, funding acquisition, supervision, reviewing and editing; U.Y.: reviewing and editing. All authors have read and agreed to the published version of the manuscript.

Funding: This research received no external funding.

Conflicts of Interest: The authors declare no conflict of interest.

List of Abbreviations

API	American petroleum institute
CCEOR	Chemical enhanced oil recovery
cm	Centimeter
cP	Centipoise
CuO	Cupric oxide
CEOR	Enhanced oil recovery
g	Grams
HPAM	Partially hydrolyzed polyacrylamide
HPHT	High pressure—high temperature
mL	Milliliter
nm	Nanometer
NPs	Nanoparticles
ONGC	Oil and natural gas corporation

List of Symbols

K	Consistency (Pa·s^n)
n	Flow behavior index (dimensionless)
S_{oi}	Initial oil saturation
$\overline{d}_p$	Particle size
S_{or}	Residual oil saturation
I	Scaling coefficient
γ	Shear rate (s^{-1})
τ	Shear stress (Pa)
τ_o	Yield stress (Pa)

References

1. Medina, O.E.; Olmos, C.; Lopera, S.H.; Cortes, F.B.; France, C.A. Nanotechnology Applied to Thermal Enhanced Oil Recovery Processes: A Review. *Energies* **2019**, *12*, 4671. [CrossRef]
2. Gbadamosi, A.O.; Junin, R.; Manan, M.A.; Agi, A.; Yusuff, A.S. An overview of chemical enhanced oil recovery: Recent advances and prospects. *Int. Nano Lett.* **2019**, *9*, 1–32. [CrossRef]
3. Corredor, L.M.; Husein, M.M.; Maini, B.B. A review of polymer nanohybrids for oil recovery. *Adv. Colloid Interface Sci.* **2019**, *272*, 102018. [CrossRef] [PubMed]
4. Lake, L.W. *Enhanced Oil Recovery*; Prentice Hall: Englewood Cliffs, NJ, USA, 1989.
5. Brundred, L.L.; Brundred, L.L., Jr. Economics of Water Flooding. *J. Pet. Technol.* **1955**, *7*, 12–17. [CrossRef]
6. Zhao, D.Z.; Wang, J.; Gates, I.D. An evaluation of enhanced oil recovery strategies for a heavy oil reservoir after cold production with sand. *Int. J. Energy Res.* **2015**, *10*, 1355–1365. [CrossRef]
7. Li, M.; Zeron, L.R.; Balcom, B. Polymer Flooding Enhanced Oil Recovery Evaluated with Magnetic Resonance Imaging and Relaxation Time Measurements. *Energy Fuels* **2017**, *31*, 4904–4914. [CrossRef]
8. Pearson, J.R.A.; Tarcy, P.M.J. Models for Flow of Non-Newtonian and Complex Fluids Through Porous Media. *J. Non-Newton. Fluid Mech.* **2002**, *102*, 447–473. [CrossRef]
9. Maurya, N.K.; Kushwaha, P.; Mandal, A. Studies on interfacial and rheological properties of water soluble polymer grafted nanoparticle for application in enhanced oil recovery. *J. Taiwan Inst. Chem. Eng.* **2017**, *70*, 319–330. [CrossRef]
10. Lambert, F.; Rinaudo, M. On the thermal stability of xanthan gum. *Polymer* **1985**, *26*, 1549–1553. [CrossRef]
11. Abdelhady, A.A. Influence of clay content on surfactant-polymer flooding for an Egyptian oil field. *J. Geol. Geophys.* **2017**, *6*, 1–7.
12. Kumar, S.; Jain, R.; Chaudhary, P.; Mahto, V. Development of inhibitive water based drilling fluid system with synthesized graft copolymer for reactive Indian shale formation. In Proceedings of the SPE Oil and Gas India Conference and Exhibition, Mumbai, Maharashtra, 4 April 2017.
13. Maia, A.M.S.; Borsali, R.; Balaban, R.C. Comparison between a Polyacrylamide and a Hydrophobically Modified Polyacrylamide Flood in a Sandstone Core. *Mater. Sci. Eng. C* **2009**, *29*, 505–509. [CrossRef]
14. Samanta, A.; Ojha, K.; Sarkar, A.; Mandal, A. Mobility Control and Enhanced Oil Recovery Using Partially Hydrolysed Polyacrylamide (PHPA). *Int. J. Oil Gas Coal Technol.* **2013**, *6*, 245–258. [CrossRef]
15. Tie, L.; Yu, M.; Li, X.; Liu, W.; Zhang, B.; Chang, Z.; Zheng, Y. Research on polymer solution rheology in polymer flooding for Qikou reservoirs in a Bohai Bay oilfield. *J. Petrol. Explor. Prod. Technol.* **2019**, *9*, 703–715. [CrossRef]
16. Yadav, U.S.; Kumar, H.; Roy, V.; Juyal, S.; Tripathi, A.; Shanker, A. Experimental evaluation of partially hydrolyzed polyacrylamide and silica nanoparticles solutions for enhanced oil recovery. *J. Petrol. Explor. Prod. Technol.* **2020**, *10*, 1–6. [CrossRef]
17. Chaudhary, P.; Kumar, S. Polymer and its Role in EOR and Water shut-off Process. *J. Basic Appl. Eng. Res.* **2016**, *3*, 717–720.
18. Xin, X.; Yu, G.; Chen, Z.; Wu, K.; Dong, X.; Zhu, Z. Effect of Polymer Degradation on Polymer Flooding in Heterogeneous Reservoirs. *Polymers* **2018**, *10*, 857. [CrossRef]
19. Al-Shammari, B.; Al-Fariss, T.; Al-Seailm, F.; Elleithy, R. The effect of polymer concentration and temperature on the rheological behavior of metallocene linear low density polyethylene (mLLDPE) solutions. *J. King Saud Univ.-Eng. Sci.* **2011**, *23*, 9–14. [CrossRef]
20. Maghzi, A.; Mohammadi, S.; Ghazanfari, M.H.; Kharrat, R.; Masihi, M. Monitoring wettability alteration by silica nanoparticles during water flooding to heavy oils in a five-spot systems: A pore level investigation. *J. Exp. Therm. Fluid Sci.* **2012**, *40*, 168–176. [CrossRef]
21. Ponmani, S.; William, J.K.M.; Samuel, R.; Nagarajan, R.; Sangwai, J.S. Formation and Characterization of Thermal and Electrical Properties of Cuo and Zno Nanofluids in Xanthan Gum. *Colloids Surf. A Physicochem. Eng. Asp.* **2014**, *443*, 37–43. [CrossRef]
22. William, J.K.M.; Ponmani, S.; Samuel, R.; Nagarajan, R.; Sangwai, J.S. Effect of CuO and ZnO nanofluids in xanthan gum on thermal, electrical and high pressure rheology of water-based drilling fluids. *J. Pet. Sci. Eng.* **2014**, *117*, 15–27. [CrossRef]

23. Kumar, N.; Kumar, A.; Kumar, S. Effect of synthesized AMPS-g-clay/CuO NanoComposite on WBDFS for challenging formations. In Proceedings of the IADC/SPE Asia Pacific Drilling Technology Conference and Exhibition, Bangkok, Thailand, 24 August 2018.
24. Shah, P.R. *Investigation of Thermodynamic Properties of Metal-Oxide Catalysts*; AAI3328649; ProQuest: Philadelphia, PA, USA, 2008.
25. Murov, J.S. *Experiments in General Chemistry*, 6th ed.; Cengage Learning: Stanford, CA, USA, 2014.
26. Clugston, J.M.; Flemming, R. *Advanced Chemistry*, revised ed.; OUP Oxford: New York, NY, USA, 2000.
27. Wei, B.; Zeron, R.; Rodrigue, D. Oil displacement mechanisms of viscoelastic polymers in enhanced oil recovery (EOR): A review. *J. Petrol. Explor. Prod. Technol.* **2014**, *4*, 113–121. [CrossRef]
28. Gou, S.; Liu, M.; Ye, Z.; Zhou, L.; Jiang, W.; Cai, X.; He, Y. Modification of a nicotinic acid functionalized water-soluble acrylamide sulfonate copolymer for chemically enhanced oil recovery. *J. Appl. Polym. Sci.* **2014**, *131*, 1–9. [CrossRef]
29. Tiwari, R.; Kumar, S.; Husein, M.M.; Rane, P.M.; Kumar, N. Environmentally benign invert emulsion mud with optimized performance for shale drilling. *J. Pet. Sci. Eng.* **2020**, *186*, 106791. [CrossRef]
30. Akhlaghinia, M.; Torabi, F.; Chain, C.W. Experimental investigation of temperature effect on three-phase relative permeability isoperms in heavy oil systems. *Fuel* **2014**, *118*, 281–290. [CrossRef]
31. Sarmha, S.; Gogoi, S.B.; Jagatheesan, K.; Hazarika, K. Formulation of a combined low saline water and polymer flooding for enhanced oil recovery. *Int. J. Ambient Energy* **2019**, 1–9. [CrossRef]
32. Dardir, M.M.; Ibrahime, S.; Soliman, M.; Desouky, S.D.; Hafiz, A.A. Preparation and evaluation of some esteramides as synthetic based drilling fluids. *Egypt. J. Pet.* **2014**, *23*, 35–43. [CrossRef]
33. Kumar, S.; Thakur, A.; Kumar, N.; Husein, M.M. A novel oil-in-water drilling mud formulated with extracts from Indian mango seed oil. *Pet. Sci.* **2020**, *17*, 196–210. [CrossRef]
34. Carlino, S.; Hudson, M.J. A thermal decomposition study on the intercalation of Tris (oxalato) ferrate, trihydrate into a layered (MG AL) double hydroxide. *Solid State Ion.* **1998**, *110*, 1–2. [CrossRef]
35. Prinetto, F.; Ghiotti, G.; Graffin, P.; Tichit, D. Synthesis and characterization of sol-gel Mg/Al and Ni/Al layered double hydroxides and comparison with co-precipitated samples. *Microporous Mesoporous Mater.* **2000**, *39*, 1–2. [CrossRef]
36. Singh, J.; Kaur, G.; Rawat, M. A Brief Review on Synthesis and Characterization of Copper Oxide Nanoparticles and its Applications. *J. Bioelectron. Nanotechnol.* **2016**, *1*, 9.
37. Kumar, S.; Sundariyal, P.; Kumar, N. Formulation of inhibitive water based mud system with synthesized graft copolymer: A novel approach to mitigate the wellbore instability problems in shale formation. In Proceedings of the Abu Dhabi International Petroleum Exhibition & Conference, Abu Dhabi, UAE, 13 November 2017.
38. Al-Shakry, B.; Shiran, B.S.; Skauge, T.; Skauge, A. Enhanced Oil Recovery by Polymer Flooding: Optimizing Polymer Injectivity. In Proceedings of the SPE Kingdom of Saudi Arabia Annual Technical Symposium and Exhibition, Damman, Saudi Arabia, 16 August 2018.
39. Shojaeefard, M.H.; Boyaghchi, F.A. Studies on the influence of various blade outlet angles in a centrifugal pump when handling viscous fluids. *Am. J. Appl. Sci.* **2007**, *4*, 718–724.
40. Jha, P.K.; Mahto, V.; Saxena, V.K. Study the rheological and filtration properties of oil-in-water emulsion for its application in oil and gas well drilling. *Arab. J. Sci. Eng.* **2016**, *41*, 25–30.
41. Kumar, S.; Chaurasia, S.; Sundriyal, P.; Gautam, S. Synthesis & Evaluation of synthesized PAA/AMPS-g-Sesbania Gum Graft Copolymer in Water Based Drilling Mud System for Mitigation of Borehole Instability in Conventional and Troublesome Formations. In Proceedings of the SPE/IADC Middle East Drilling Technology Conference and Exhibition, Abu Dhabi, UAE, 29 January 2018.
42. Nezhad, S.S.K.; Cheraghian, G. Mechanisms behind injecting the combination of nano-clay particles and polymer solution for enhanced oil recovery. *Appl. Nanosci.* **2016**, *6*, 923–931. [CrossRef]
43. Nezhad, S.S.K.; Cheraghian, G.; Roayaei, E.; Tabatabaee, H.; Karambeigi, M.S. Improving heavy oil recovery in the polymer flooding process by utilizing hydrophilic silica nanoparticles. *Energy Sources Part A Recovery Util. Environ. Eff.* **2017**, 1–10.
44. Cheraghian, G.; Nezhad, S.S.K. Experimental Investigation of Polymer Solutions Used in Enhanced Oil Recovery—Thermal properties Improved by Nanoclay. In Proceedings of the 77th EAGE Conference and Exhibition, Madrid, Spain, 1 June 2015.

45. Nafchi, H.R.; Abdouss, M.; Najafi, S.K.; Gargari, R.M.; Mazhar, M. Effects of nano-clay particles and oxidized polypropylene polymers on improvement of the thermal properties of wood plastic composite. *Maderas, Cienc. Tecnol.* **2015**, *17*, 45–54. [CrossRef]
46. Rapoport, L.; Leas, W. Properties of linear waterfloods. *J. Pet. Technol.* **1953**, *5*, 139–148. [CrossRef]
47. Esmaeili, S.; Sarma, H.; Harding, T.; Maini, B.B. Review of the effect of temperature on oil-water relative permeability in porous rocks of oil reservoirs. *Fuel* **2019**, *237*, 91–116. [CrossRef]
48. Kumar, S.; Esmaeili, S.; Sarma, H.; Maini, B. Can Effects of Temperature on Two-Phase Gas/Oil-Relative Permeabilities in Porous Media Be Ignored? A Critical Analysis. *Energies* **2020**, *13*, 3444. [CrossRef]